Non-collinear high-order harmonic generation by three interfering laser beams

M. Negro,[1,*] **M. Devetta,**[1] **D. Faccialá,**[2] **A.G. Ciriolo,**[2] **F. Calegari,**[1] **F. Frassetto,**[3] **L. Poletto,**[3] **V. Tosa,**[4] **C. Vozzi,**[1] **and S. Stagira**[2]

[1] *Istituto di Fotonica e Nanotecnologie - CNR - Milano, Italy*
[2] *Department of Physics, Politecnico di Milano, Milan, Italy*
[3] *Istituto di Fotonica e Nanotecnologie - CNR - Padova, Italy*
[4] *National Institute for R&D Isotopic and Molecular Technologies, Cluj-Napoca, Romania*

[*]*matteo.negro@polimi.it*

Abstract: High order harmonic generation (HHG) has shown its impact on several applications in Attosecond Science and Atomic and Molecular Physics. Owing to the complexity of the experimental setup for the generation and characterization of harmonics, as well as to the large computational costs of numerical modelling, HHG is generally performed and modelled in collinear geometry. Recently, several experiments have been performed exploiting non-collinear geometry, such as HHG in a grating of excited molecules created by crossing beams. In such studies, harmonics were observed at propagation directions different from those of the driving pulses; moreover the scattered harmonics were angularly dispersed.

In this work we report on a new regime of HHG driven by multiple beams, where the harmonics are generated by three synchronized, intense laser pulses organized in a non-planar geometry. Although the configuration we explore is well within the strong-field regime, the scattered harmonics we observe are not angularly dispersed.

References and links

1. F. Calegari, M. Lucchini, M. Negro, C. Vozzi, L. Poletto, O. Svelto, S. De Silvestri, G. Sansone, S. Stagira, and M. Nisoli, "Temporal gating methods for the generation of isolated attosecond pulses," J. Phys. B Atom. Molec. Opt. Phys. **45**, 074002 (2012)
2. E. Goulielmakis, M. Schultze, M. Hofstetter, V. S. Yakovlev, J. Gagnon, M. Uiberacker, A. L. Aquila, E. M. Gullikson, D. T. Attwood, R. Kienberger, F. Krausz, and U. Kleineberg, "Single-cycle nonlinear optics," Science **320**, 1614-1617 (2008).
3. J. A. Wheeler, A. Borot, S. Monchoce, H. Vincenti, A. Ricci, A. Malvache, R. Lopez-Martens, and F. Quere, "Attosecond lighthouses from plasma mirrors," Nature Phot. **6**, 829-833 (2012).
4. J. Itatani, J. Levesque, D. Zeidler, H. Niikura, H. Pepin, J. Kieffer, P. Corkum, and D. Villeneuve, "Tomographic imaging of molecular orbitals," Nature **432**, 867-871 (2004).
5. C. Vozzi, M. Negro, F. Calegari, G. Sansone, M. Nisoli, S. De Silvestri, and S. Stagira, "Generalized molecular orbital tomography," Nature Phys. **7**, 822-826 (2011).
6. D. Shafir, Y. Mairesse, D. M. Villeneuve, P. B. Corkum and N. Dudovich, "Atomic wavefunctions probed through strong-field light-matter interaction," Nature Phys. **5**, 412-416 (2009).
7. O. Smirnova, Y. Mairesse, S. Patchkovskii, N. Dudovich, D. Villeneuve, P. Corkum and M. Y. Ivanov, "High harmonic interferometry of multi-electron dynamics in molecules," Nature **460**, 972-977 (2009).

8. A. V. Birulin, V. T. Platonenko, and V. V. Strelkov, "High-order harmonic generation in colliding beams," Quantum Electron. **26**, 377-378 (1996).

9. S. V. Fomichev, P. Breger, B. Carré, P. Agostini, and D. F. Zaretsky, "Non-collinear high-harmonic generation," Laser Phys. **12**, 383-388, (2002).

10. Y. Mairesse, D. Zeidler, N. Dudovich, M. Spanner, J. Levesque, D. M. Villeneuve, and P. B. Corkum, "High-order harmonic transient grating spectroscopy in a molecular jet," Phys. Rev. Lett. 100, 143903 (2008).

11. H. J. Wörner, J. B. Bertrand, B. Fabre, J. Higuet, H. Ruf, A. Dubrouil, S. Patchkovskii, M. Spanner, Y. Mairesse, V. Blanchet, E. Mével, E. Constant, P. B. Corkum, and D. M. Villeneuve, "Conical intersection dynamics in NO_2 probed by homodyne high-harmonic spectroscopy," Science **334**, 208-212 (2011).

12. A. Rupenyan, J. B. Bertrand, D. M. Villeneuve, and H. J. Wörner, "All-optical measurement of high-harmonic amplitudes and phases in aligned molecules," Phys. Rev. Lett. **108**, 033903 (2012).

13. J. B. Bertrand, H. J. Wörner, H.-C. Bandulet, É. Bisson, M. Spanner, J.-C. Kieffer, D. M. Villeneuve, and P. B. Corkum, "Ultrahigh-order wave mixing in noncollinear high harmonic generation," Phys. Rev. Lett. **106**, 023001 (2011).

14. C. M. Heyl, P. Rudawski, F. Brizuela, S. N. Bengtsson, J. Mauritsson, and A. L'Huillier, "Macroscopic effects in noncollinear high-order harmonic generation," Phys. Rev. Lett. **112**, 143902 (2014)

15. C. M. Heyl, S. N. Bengtsson, S. Carlström, J. Mauritsson, C. L. Arnold and A. L'Huillier, "Noncollinear optical gating," New J. Phys. **16** 052001 (2014).

16. J. P. Farrell, L. S. Spector, M. B. Gaarde, B. K. McFarland, P. H. Bucksbaum, and M. Gühr, "Strongly dispersive transient Bragg grating for high harmonics," Opt. Lett. **35**, 2028-2030 (2010).

17. D. Romanov, A. Filin, R. Compton, and R. Levis, "Phase matching in femtosecond BOXCARS," Opt. Lett. **32**, 3161-3163 (2007).

18. A. Fleischer and N. Moiseyev, "Attosecond laser pulse synthesis using bichromatic high-order harmonic generation," Phys. Rev. A **74**, 053806 (2006).

19. G. Sansone, C. Vozzi, S. Stagira, and M. Nisoli, "Nonadiabatic quantum path analysis of high-order harmonic generation: Role of the carrier-envelope phase on short and long paths," Phys. Rev. A **70**, 013411 (2004).

1. Introduction

High order harmonic generation (HHG) from gaseous media is a powerful tool exploited in a wide number of applications, ranging from the generation of attosecond pulses [1–3] to the investigation of the structure and the dynamics of atomic and molecular orbitals [4–7]. In such a process an intense femtosecond laser pulse is focused in a gas jet, generating extreme ultraviolet radiation collinearly with respect to the driving beam. This represents the easiest configuration which has been used both for exploring the properties of the process and for generating coherent radiation in the XUV and X-rays spectral ranges. However, the exploitation of high harmonics generated in collinear geometry, as well as their characterization, requires the use of laser-blind detectors or the selective attenuation of the laser radiation with unavoidable reduction of the XUV energy. Birulin et al. proposed for the first time non collinear HHG with counter-propagating beams, suggesting a method for considerably increasing the conversion efficiency of the process [8]. Later on, Fomichev et al. [9] experimentally demonstrated an alternative route, involving the exploitation of two almost co-propagating beams crossing at a small angle and interfering in the medium. In the last years, HHG from interfering laser beams has been addressed by several more works, considering different configurations. For instance, it was proposed to induce a grating of excited population by low-intensity beams and to generate high harmonics with only one strong pulse, with the aim of efficiently detecting the signal coming from a very small excited fraction of the target [10–12]. Another case was investigated by Bertrand et al., who employed two non-collinear intense driving beams of different wavelengths to generate non-collinear HHG [13]. Heyl et al., by following the same approach, demonstrated the exploitation of non collinear HHG for isolating spatially dispersed single attosecond pulses [14, 15]. Finally, Farrell et al. have shown that harmonics generated by one strong pulse can be spatially dispersed by a Bragg grating produced by two counter-propagating intense laser beams [16]. In all these studies, harmonics were detected at propagation directions different from the ones of the driving beams. Moreover the investigations reported in [13–16], performed in the strong interaction regime with multiple intense beams, showed that the scattered harmonic
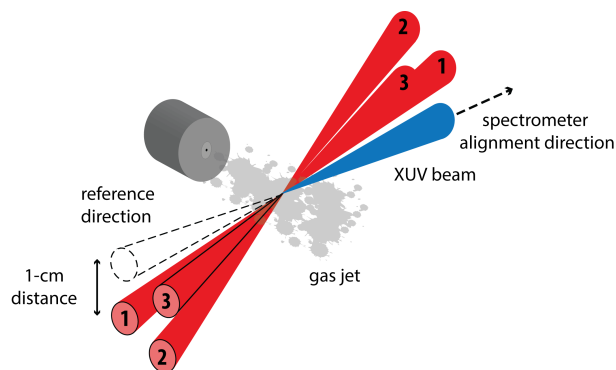
Fig. 1. Experimental setup: three laser beams are focused in the gas jet in the BoxCARS configuration; high harmonic radiation emerges from the interaction region along a fourth (reference) direction aligned to the XUV spectrometer.

radiation was angularly dispersed, namely different scattered harmonics propagated in different directions. In this work we propose a novel configuration for HHG by multiple intense beams, where the harmonic radiation is generated by three synchronized, intense and ultrashort laser pulses arranged in the so called BoxCARS geometry [17]. The case we explore is well within the strong-field regime, namely each of the three pulses is able to drive HHG; however, with respect to previous studies performed in similar conditions, the scattered harmonics we observe are not angularly dispersed.

2. Experimental setup

The three pulses exploited in the experiment were obtained starting from a Ti:Sapphire amplified laser source (800 nm, 60 fs, 120 mJ maximum pulse energy, 10 Hz repetition rate). The output of the laser source was split into four arms with identical energy (0.3 mJ each); the split was achieved by means of three 50:50 beamsplitters and the beams had a diameter of about 5 mm FWHM. Temporal synchronization among the pulses was achieved by means of remotely controlled high-resolution delay stages. The fourth beam (hereafter called reference beam) was used as a reference for the output direction of the BoxCARS configuration. The beams were separately sent to a vacuum chamber, where they were re-combined and aligned to be parallel by using two masks with four holes on the vertices of a square having 1-cm sides. The masks were located several meters away from each other to ensure a good parallelism. The beams were focused into a gas jet produced by a pulsed valve at 4-bars backing pressure, operating at 10 Hz and synchronized to the laser pulses. Focusing was achieved by means of a 20-cm focal length spherical mirror, which yields a peak intensity in the focal position of about 10^{14} W/cm^2 for each beam. The incidence angle on the mirror was kept as low as $4°$, to prevent the occurrence of aberrations and a subsequent distortion of the spatial profile of the beams in the focus. The scheme of this configuration as it was used in the experiment is shown in Fig. 1.

The reference beam was aligned to the entrance of a flat-field XUV spectrometer, coupled to a micro-channel plate and a CCD camera. Initially, as a test of alignment, only the reference beam was sent into the chamber and harmonic emission was observed in the spectral region between 16 and 36 eV in xenon and krypton and between 25 and 50 eV in argon. Synchronization and spatial overlap among the remaining beams was obtained by suppressing separately the harmonic emission of the reference in presence of each of the other three beams. Indeed, when the beams were overlapped, the high intensity in the focus led to a higher plasma density which
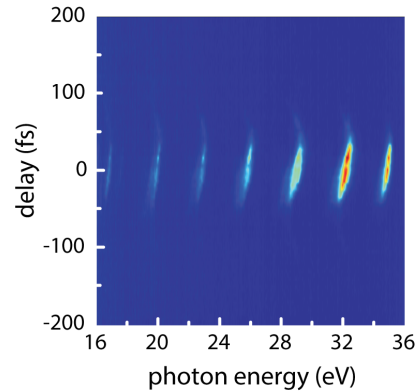
Fig. 2. Scan of the scattered harmonics spectra acquired in krypton as a function of the delay of one of the laser pulses with respect to the other two, which are kept synchronized.

destroyed the good phase-matching conditions for harmonic generation. After optimization of the beam alignment, the reference beam was blocked and harmonic emission was detected in the direction of the (blocked) reference one, due to the interaction among the three remaining beams. The diffracted harmonic signal was maximized by adjusting the aperture of irises on each of the beams, and set to a size of the order of 3 mm. The harmonic radiation has been studied as a function of the delay between the three pulses in several gases (xenon, krypton, argon).

3. Experimental results and discussion

Figure 2 shows a scan of the scattered harmonics spectra acquired in krypton as a function of the delay of one of the laser pulses with respect to the other two (which are kept synchronized). Each spectrum was integrated over 100 laser shots. Out of synchronization no harmonic signal is detected, while at temporal overlap a strong harmonic emission appears in the reference direction; weak harmonics can be also detected outside the temporal overlap, in particular for positive delays: this can be attributed to the plasma grating induced by the two synchronized pulses. One can notice that, in the spectral region under investigation, all the odd harmonic orders of the fundamental radiation (11th, 13th, 15th, 17th, 19th) are present, so the XUV radiation is not angularly dispersed, differently from the cases reported in other works [10–16]. The observation of high harmonics in the reference direction can be attributed to the interference of the nonlinear dipoles originating from the three interacting beams in the excited medium. The details of the theoretical interpretation will be provided in the *Modelling* section.

It is worth noting that the peak positions of the harmonics as well as their width slightly change with the delay; such behavior could be attributed to the effect of ionization or to volume effects related to the spatio-temporal evolution of the interaction among the beams in the gaseous medium.

We performed the same delay scan in both xenon and argon and observed the same behavior; Fig. 3 shows a comparison between the harmonic spectra generated in the reference direction at synchronization between the beams in the three gases. The first feature one can notice from Figs. 3(a) and 3(b) that harmonics in argon are broader than their counterpart generated in krypton and xenon. This can be attributed to the different generation conditions. Indeed, the intensities and focusing conditions, (optimized by tuning the irises outside the vacuum chamber) used for the three gases were different, due to their different ionization potentials. Moreover,

a blue-shift is observed in harmonics generated in xenon with respect to krypton (Fig. 3(a)). Calculations have shown that this effect can be fully accounted for a single atom approach (without taking into account propagation of the fundamental field in the plasma generated by the three pulses), owing to the different times at which harmonic generation occurs in the two gases. Indeed, harmonics in xenon are generated earlier in the pulse, where one can observe a rapid increase of the field intensity from cycle to cycle[, while in krypton the harmonic emission occurs closer to the pulse center, where the variation of the field intensity is lower. In the next section we will provide a simple theoretical description of the process.

4. Modelling

The generation of high-order harmonics by three interfering beams in a gaseous medium can be modeled by different approaches; we will exploit here a simple one, based on photon energy and momentum conservation, and a more sophisticated model, based on the determination of the nonlinear dipole emission by an adiabatic saddle-point approximation of the Lewenstein model.

Harmonic emission can be understood as a high-order noncollinear wave mixing process [13, 18]; in such a case, the emission obeys to the photon momentum and energy conservation laws:

$$\begin{cases} \hbar\omega_X = \sum_i n_i\hbar\omega_i \\ \hbar\mathbf{k}_X = \sum_i n_i\hbar\mathbf{k}_i \\ \sum_i n_i = 2m+1 = q, \; n_i \in \mathbb{Z}, \; m \in \mathbb{N} \end{cases} \qquad (1)$$

where ω_i are the frequencies and $\mathbf{k}_i$ the wavevectors of the photons carried by the foundamental beams, n_i the number of absorbed photons from the beams and ω_X, $\mathbf{k}_X$ energy and wavevector of the emitted XUV photon, respectively. As can be seen in the previous formulae, the net number of absorbed photons must be odd in order to have XUV emission and $q = 2m+1$ is the order of the produced harmonic emission. In the experimental configuration we adopted, the
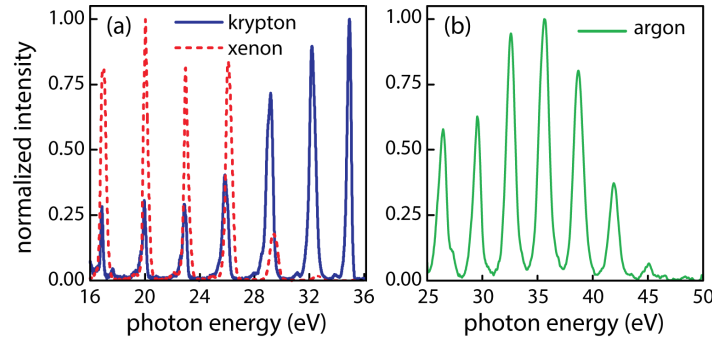

Fig. 3. a) Harmonic spectra generated in the reference direction in xenon (blue solid line) and krypton (red dashed line) at synchronization of the three beams. b) Harmonic spectrum generated in the reference direction in argon (green solid line) at synchronization of the three beams.
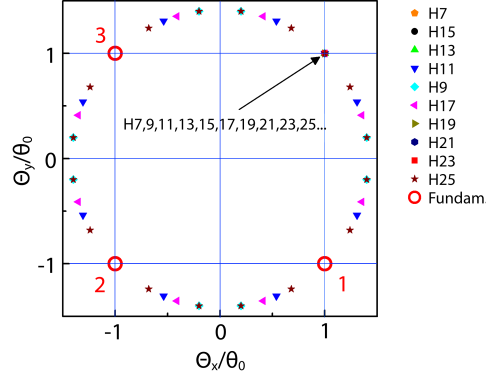
Fig. 4. Predicted emission directions of harmonics generated by three laser beams (shown as empty circles) positioned at the three vertices of a square, for orders ranging from 7th to 25th. Harmonics are not angularly dispersed only in the three driving directions (not shown) and in the reference direction (indicated by an arrow). Θ_x and Θ_y are the angles formed with x and y axes; θ_0 is the angle formed by the driving beams with the same axes.

previous relations can be written as:

$$\begin{cases} \omega_X = q\omega_0 \\ \\ \mathbf{k}_X = qk_{0z}\mathbf{u}_z + k_{0\perp}\left[(n_3 - n_2 - n_1)\mathbf{u}_x + (n_1 - n_2 - n_3)\mathbf{u}_y\right] \end{cases} \tag{2}$$

where ω_0 is the fundamental laser frequency, $k_0 = |\mathbf{k}_i| = \omega_0/c$, $k_{0z} = k_0\cos\alpha$, $k_{0\perp} = k_0\sin\alpha/\sqrt{2}$, and α is the angle formed by the three interacting beams with the longitudinal axis z, which amount to about $4°$ in our experimental conditions. After some algebra, one finds that the latter equations reduce to:

$$\begin{cases} \dfrac{2n_1^2 + 2n_1 n_2 + n_2^2}{2n_1 + n_2} = q \\ \\ n_3 = q - n_1 - n_2 \end{cases} \tag{3}$$

It can be easily shown that the emission direction of the generated harmonics always form an angle α with the z axis; this feature is clearly observed in Fig. 4, which displays the theoretical emission directions of the harmonics generated by three identical beams for orders ranging from the 7th to 25th. In particular, angularly dispersed harmonics are expected to be generated along a phase matching cone passing through the directions of the three generating foundamental beams. It is worth noting that, besides harmonic generation along the direction of the driving beams (not shown), nondispersed (i.e. copropagating) harmonics are also expected along the reference direction. These harmonics correspond to the conditions $n_1 = q$, $n_2 = -q$, $n_3 = q$.

An interesting feature observed in Fig. 4 is that some harmonics are only generated along the driving and the reference directions, whereas some others are generated along additional directions. The reason for this peculiar behavior can be understood by finding the solutions of Eq. (3); in particular, by expressing n_1 as a function of the other quantities, one finds:

$$n_1 = \frac{(q - n_2) \pm \sqrt{q^2 - n_2^2}}{2}. \tag{4}$$

It follows that q, n_2 and $\Delta = \sqrt{q^2 - n_2^2}$ must belong to a Pythagorean triple in order to give integer values for n_1 (and for n_3); in particular q must be the largest number of the triple (hypotenuse). Some harmonic orders, like $q = 3, 7, 9, 11, 19, 21, 23, ...$, are not "hypotenuse" of a Pythagorean triple. As can be seen in Fig. 4, for those orders only the trivial solutions corresponding to harmonic generation along the reference or along the three driving beam directions are possible. For orders $q = 5, 13, 17, ...$, belonging to a primitive Pythagorean triple, and for orders $q = 15, 39, 51, ...$, belonging to triples proportional to a primitive one, 8 distinct additional emission directions are found besides the 4 trivial ones. As an example, we show in Table 1 a summary of the emission processes expected for harmonic 13th. It is worth noting that orders $q = 25, 85, ...$ are "hypotenuse" of two different Pythagorean triples; in such cases, 16 distinct additional emission directions should be observed besides the 4 trivial ones.

Table 1. Nonlinear wave mixing processes corresponding to generation of harmonic 13th driven by three fundamental laser pulses with identical frequency.

n_1	n_2	n_3	$k_{X,x}^{(13)}/qk_{0x}$	$k_{X,y}^{(13)}/qk_{0y}$	$k_{X,z}^{(13)}/qk_{0z}$
13	0	0	-1	1	1
0	13	0	-1	-1	1
0	0	13	1	-1	1
13	-13	13	1	1	1
10	5	-2	-17/13	7/13	1
-2	5	10	7/13	-17/13	1
3	12	-2	-17/13	-7/13	1
-2	12	3	-7/13	-17/13	1
15	-5	3	-7/13	17/13	1
3	-5	15	17/13	-7/13	1
15	-12	10	7/13	17/13	1
10	-12	15	17/13	7/13	1

Although the wave mixing modelling easily explains the generation process occurring in the interaction region, it does not provide an accurate description of the microscopic mechanisms at the base of the process. In particular, it is well known that high order harmonic generation strongly depends on the behavior of quantum electron trajectories in the continuum; moreover phase matching effects dominate the harmonic emission yield. These two aspects are not taken into account by the wave mixing model, which considers harmonic generation as perfectly phase-matched and independent on the microscopic phenomena taking place in the emission process. For these reasons, a more sophisticated model is required for a deeper understanding of the harmonic generation driven by multiple beams. It must be noted that a complete numerical model, based onto the solution of the Schrödinger equation in a tridimensional domain and for ultrashort driving pulses, is computational demanding. Hence we limited our investigation by modelling the nonlinear dipole emission from the interaction region with a saddle-point adiabatic approximation of the Lewenstein model.

In particular, the three interacting laser beams are treated as continuous plane waves, with the resulting electric field given by:

$$E = A \left\{ \exp\left[i\left(\mathbf{k}_1 \cdot \mathbf{r}\right)\right] + \exp\left[i\left(\mathbf{k}_2 \cdot \mathbf{r}\right)\right] + \exp\left[i\left(\mathbf{k}_3 \cdot \mathbf{r}\right)\right] \right\} \exp\left[-i\omega_0 t\right] \quad (5)$$

After some trivial algebra, one finds the expression of the electric field in the experimental

conditions, given by:

$$E = A\rho(x,y) \exp[i\phi(x,y)] \exp[i(k_{0z}z - \omega_0 t)] \tag{6}$$

where

$$\begin{cases} \rho^2(x,y) = 4\cos^2[k_{0\perp}(x-y)] + 4\cos[k_{0\perp}(x+y)]\cos[k_{0\perp}(x-y)] + 1 \\ \\ \phi(x,y) = \arctan\left[-\dfrac{\sin[k_{0\perp}(x+y)]}{2\cos[k_{0\perp}(x-y)] + \cos[k_{0\perp}(x+y)]} \right] \end{cases} \tag{7}$$

The non linear dipole at the q-th order is determined as a function of the transverse coordinates by adiabatic saddle point simulations [19]; in this calculation the saddle-point approximation allows to disentangle the contributions from short and long quantum path, hence providing a deeper understanding of the process. The non linear dipole is then given by:

$$d_{s/l}^{(q)}(x,y) = SP_{s/l}\{A\rho(x,y)\} \exp[iq\phi(x,y)] \exp[iqk_{0z}z] \tag{8}$$

where $SP_{s/l}\{\cdot\}$ represents the adiabatic saddle-point operator determining the contribution of short/long quantum path to the dipole. The far-field harmonic intensity pattern is then given by:

$$I_{s/l}(\kappa_x, \kappa_y) \propto l^2 \left|F_{s/l}(\kappa_x, \kappa_y)\right|^2 \mathrm{sinc}^2\left(\frac{\Delta k l}{2}\right) \tag{9}$$

where l is the length of the generating medium, $\Delta k = qk_{0z} - \sqrt{q^2 k_0^2 - \kappa_x^2 - \kappa_y^2}$ and $F_{s/l}(\kappa_x, \kappa_y) = \mathscr{F}_{\kappa_x, \kappa_y}\{SP_{s/l}\{A\rho(x,y)\} \exp[iq\phi(x,y)]\}$ is the Fourier transform of the transverse non linear dipole profile.

Figure 5 shows the far-field profile of the 11th harmonic emission corresponding to short (left panel) and long (right panel) electron quantum paths; simulations are performed taking into account a 1-mm propagation inside the generating medium, but neglect neutral and plasma contribution to phase matching. Although the wave-mixing model predicts emission of the 11-th harmonic only along the driving and the reference directions, numerical simulations show that a very different pattern could be observed. In particular, the short quantum path gives
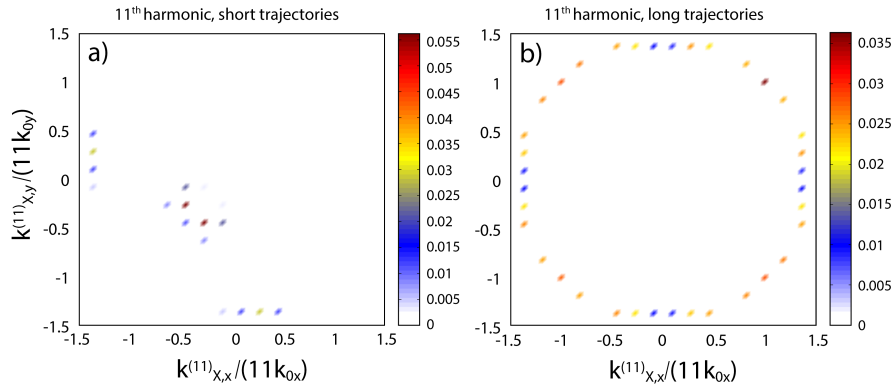

Fig. 5. Numerical simulation reporting the far-field profile of the 11th harmonic emission corresponding to short (left panel) and long (right panel) electron quantum paths. Simulations consider propagation in a 1-mm thick medium and neglect neutral and plasma contribution to the phase matching.

rise to emission towards the center of the beam configuration, whereas the long quantum path is responsible for emission in the outer region. This discrepancy between the two models is explained taking into account the finite propagation distance considered in the numerical simulations, which is of the order of the coherent length of the emission processes. Indeed it has been verified that for very long interaction regions (in the orders of several cm), predictions from the two models converge, since only the phase-matched contributions dominate the far-field pattern. However on the basis of the numerical simulations, it is expected that in a real experiment the long quantum path contribution to harmonic emission in the reference direction would prevail over the short path one.

High order harmonic generation by multiple interacting beams has shown its potentiality in a wide number of applications in HHG spectroscopy and Attosecond Science [10–16]. In a strong-field regime, previous works have shown that harmonic radiation emitted from more interfering beams is angularly dispersed. Here we show that, by exploiting three intense beams arranged in a BoxCARS configuration, we were able to detect non-dispersed harmonic emission in the direction of the fourth vertex. This outcome gives access to the study of HHG in non collinear geometry with a simpler detection scheme with respect to other configurations, providing a powerful tool to high harmonic spectroscopy of excited samples.

Acknowledgments